Supplementary Information

Nanoclay-enhanced self-healing of polyurethane–urea coatings enabled by disulfide exchange

Ronak Ansaripour, ‡ Maryam Bonyani, ‡ and Sitaraman Krishnan ⋆

Department of Chemical & Biomolecular Engineering, Clarkson University,

8 Clarkson Avenue, Potsdam, New York, USA

‡ These authors contributed equally to this work.

⋆ Corresponding author. Email: skrishna@clarkson.edu, Phone: +1 315 268 6661

S1. Estimation of gelation threshold by Flory–Stockmayer theory

The gelation behavior of the polyurethane–urea systems was analyzed using the Flory–Stockmayer framework for step-growth polymerization [1].

The stoichiometric ratio factor r is defined as the ratio of the limiting to excess initial functional-group populations, such that $0 < r \leq 1$:

$$r = \frac{\min(N_{\mathrm{A},0}, N_{\mathrm{B},0})}{\max(N_{\mathrm{A},0}, N_{\mathrm{B},0})} \tag{S1}$$

where $N_{\mathrm{A},0}$ and $N_{\mathrm{B},0}$ are the initial numbers of complementary reactive A and B functional groups, respectively. The critical extent of reaction at the gel point is then given by

$$p_{\mathrm{c}} = \frac{1}{\sqrt{r(f_{\mathrm{w,A}} - 1)(f_{\mathrm{w,B}} - 1)}} \tag{S2}$$

where $f_{\mathrm{w,A}}$ and $f_{\mathrm{w,B}}$ are the corresponding weight-average functionalities.

In the present formulations, the isocyanate component (IPDI) is difunctional, such that

$$f_{\mathrm{w,A}} = 2 \tag{S3}$$

while the nucleophilic component comprises a mixture of di- and trifunctional species. The weight-average functionality of the nucleophilic component is therefore given by

$$f_{\mathrm{w,B}} = \frac{\sum_i N_i f_i^2}{\sum_i N_i f_i} \tag{S4}$$

where N_i and f_i are the molar amount and functionality of species i.

The initial isocyanate population is given by the total number of NCO groups contributed by IPDI,

$$N_{\mathrm{A},0} = 2n_{\mathrm{IPDI}} \tag{S5}$$

while the nucleophilic population is given by the sum of hydroxyl and amine functionalities,

$$N_{\mathrm{B},0} = 2n_{\mathrm{PEG}} + 2n_{\mathrm{PDMS}} + 2n_{\mathrm{APDS}} + 3n_{\mathrm{crosslinker}} \tag{S6}$$

Using the formulation compositions in Table 4, the PUU formulation gives $N_{\mathrm{A},0} = 4.74$ mmol and $N_{\mathrm{B},0} = 4.98$ mmol, whereas the PUU-DPDS formulation gives $N_{\mathrm{A},0} = 4.72$ mmol and $N_{\mathrm{B},0} = 4.59$ mmol. These values correspond to stoichiometric ratio factors of $r = 0.952$ for PUU and $r = 0.973$ for PUU-DPDS.

Using the formulation compositions (Table 4), $f_{\mathrm{w,B}}$ is estimated to be ≈ 2.3 for PUU and ≈ 2.2 for PUU-DPDS. Incorporating the calculated stoichiometric ratio factors gives predicted critical extents of reaction of approximately $p_{\mathrm{c}} \approx 0.89$ for PUU and $p_{\mathrm{c}} \approx 0.94$ for PUU-DPDS.

These estimates indicate that gelation requires high functional-group conversion, and that partially branched but soluble species can persist below the gel threshold. This is consistent with the experimentally observed formation of viscous, processable solutions during synthesis, as well as the presence of finite sol fractions in the final materials.

It should be noted that this analysis is based on an idealized random step-growth model. In the present system, the staged synthesis route, differences in reactivity between hydroxyl and amine groups, and potential microphase segregation may influence network formation. Accordingly, the calculated values of p_{c} should be interpreted as approximate indicators of gelation behavior rather than exact predictions.

S2. Hansen solubility parameter analysis of copolymer–solvent interactions

Hansen solubility parameters (HSPs) were used to compare the relative compatibility of the segmented PUU network with selected swelling solvents. The HSP framework separates cohesive interactions into dispersion, polar, and hydrogen-bonding components, denoted as δ_{D}, δ_{P}, and δ_{H}, respectively [2]. The Hansen distance, R_{a}, between the polymer and a solvent was calculated as:

$$R_{\mathrm{a}} = \left[4(\delta_{\mathrm{D,p}} - \delta_{\mathrm{D,s}})^2 + (\delta_{\mathrm{P,p}} - \delta_{\mathrm{P,s}})^2 + (\delta_{\mathrm{H,p}} - \delta_{\mathrm{H,s}})^2\right]^{1/2} \tag{S7}$$

where subscripts p and s refer to polymer and solvent, respectively.

Because reliable HSP values for the fully reacted segmented network are not available, a composition-weighted estimate based on the dominant PEG and PDMS soft segments was used as a first-order approximation. The PEG/PDMS composition was estimated from the precursor feed ratio (Table S1) as approximately 0.23/0.77 by weight, considering only PEG and PDMS components. The effective HSP was then calculated as:

$$\delta_{i,\text{copolymer}} = w_{\text{PEG}}\delta_{i,\text{PEG}} + w_{\text{PDMS}}\delta_{i,\text{PDMS}} \tag{S8}$$

where $i = \text{D}, \text{P}, \text{H}$.

This yielded an effective copolymer HSP of:

$$(\delta_{\text{D}}, \delta_{\text{P}}, \delta_{\text{H}})_{\text{copolymer}} = (16.08,\ 2.07,\ 5.46)\ \text{MPa}^{1/2} \tag{S9}$$

Urethane/urea hard segments, IPDI-derived units, crosslinking junctions, and APDS-derived segments were not explicitly included in this calculation. These components increase polar and hydrogen-bonding contributions (urethane/urea), while the aromatic disulfide units contribute to dispersion interactions.

Table S1: Composition of PUU and PUU-DPDS formulations.

Material	PUU (g)	PUU-DPDS (g)
PEG	0.268	0.261
PDMS	0.883	0.875
Bis(4-aminophenyl) disulfide (APDS)	–	0.060
Trifunctional amine crosslinker	0.239	0.120
IPDI	0.527	0.524
Total	1.917	1.840

Table S2: Hansen solubility parameters used for solvent compatibility analysis. Values are given in $\text{MPa}^{1/2}$.

Material/solvent	δ_{D}	δ_{P}	δ_{H}	R_{a} to copolymer
Effective PEG/PDMS copolymer	16.08	2.07	5.46	–
Toluene	18.00	1.40	2.00	5.20
DMF	17.40	13.70	11.30	13.28
DMSO	18.40	16.40	10.20	15.79

The HSP values and calculated Hansen distances are summarized in Table S2. The calculated Hansen distances show that toluene is substantially closer to the PEG/PDMS-weighted copolymer composition than DMF or DMSO. The latter possess large polar and hydrogen-bonding components and are therefore expected to preferentially interact with polar hard domains rather than uniformly swell the amphiphilic network.

Accordingly, toluene was selected as the swelling solvent, as it provides a more balanced interaction with both dispersive and polar components of the system. The HSP analysis is used only as a comparative guide, as it does not capture network heterogeneity, microphase separation, or physical/topological constraints. Consequently, swelling-derived Flory–Rehner values are interpreted as apparent or effective network constraints rather than absolute covalent crosslink densities.

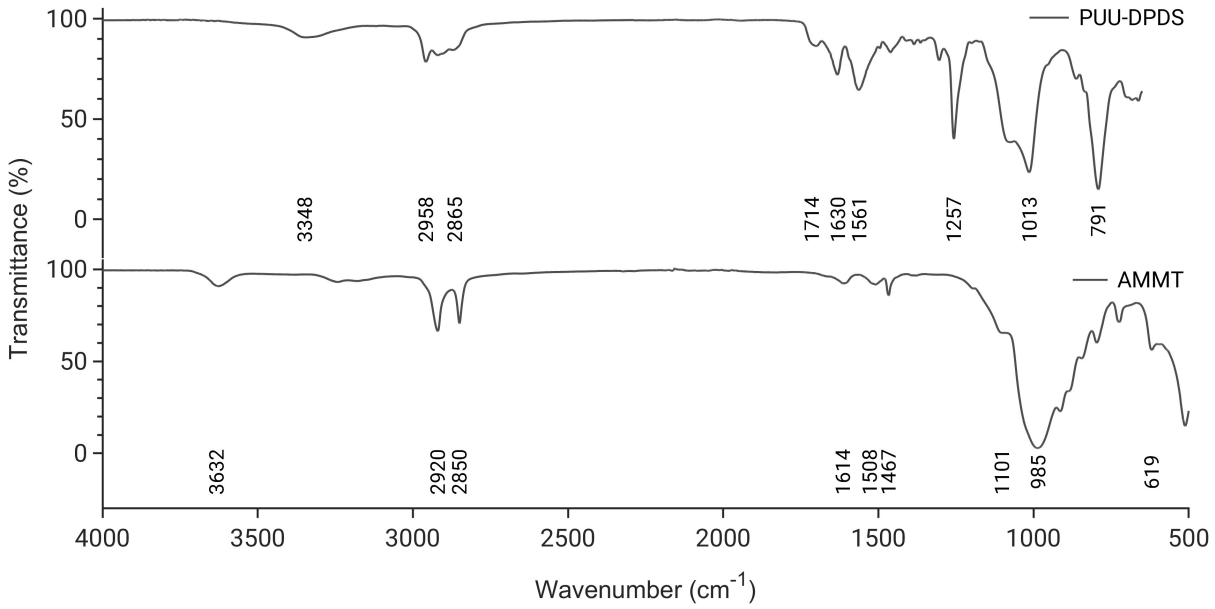

Fig. S1: ATR-FTIR spectra of the PUU-DPDS film and γ-aminopropyltriethoxysilane-functionalized montmorillonite (AMMT).

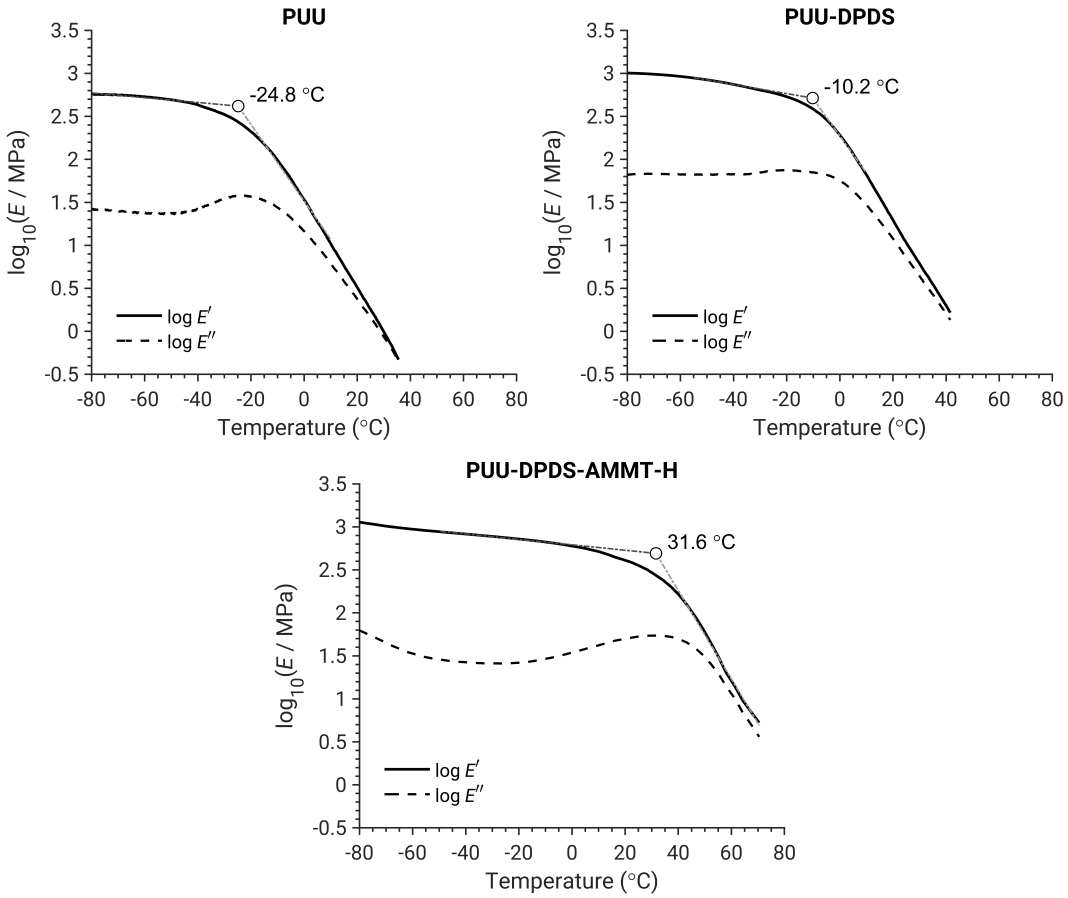

Fig. S2: Temperature-dependent dynamic mechanical analysis of PUU, PUU-DPDS, and PUU-DPDS-AMMT-H systems showing the storage modulus ($\log_{10} E'$) and loss modulus ($\log_{10} E''$) as a function of temperature. Solid lines represent $\log_{10} E'$, while dashed lines correspond to $\log_{10} E''$. The onset glass transition temperature ($T_{\mathrm{g,onset}}$) is determined from the intersection of tangential lines constructed on the $\log_{10} E'$ curves in the glassy and transition regions, as indicated by the open circles and annotated values ($-24.8\,^{\circ}\mathrm{C}$ for PUU, $-10.2\,^{\circ}\mathrm{C}$ for PUU-DPDS, and $31.6\,^{\circ}\mathrm{C}$ for PUU-DPDS-AMMT-H).

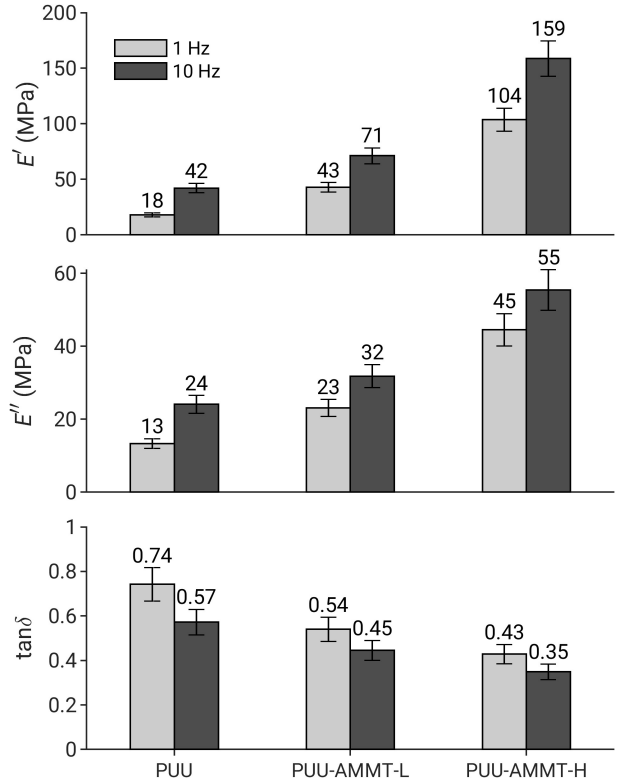

Fig. S3: Frequency sweep DMA results at ∼25 °C showing the storage modulus (E'), loss modulus (E''), and loss tangent ($\tan\delta$) of the PUU copolymer and the PUU-AMMT composite films, measured at 1 and 10 Hz.

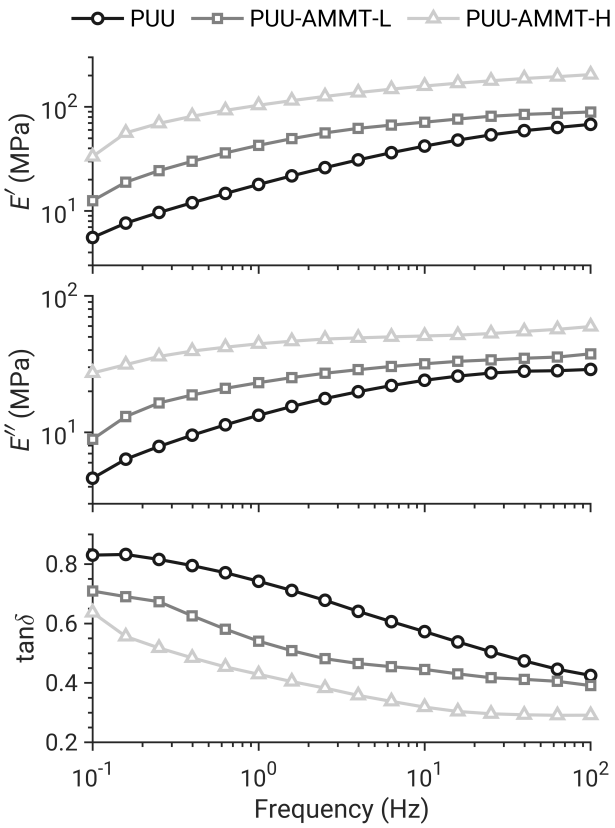

Fig. S4: Frequency-dependent viscoelastic properties of PUU-based materials obtained from dynamic mechanical analysis. ◯ = PUU, □ = PUU-AMMT-L, △ = PUU-AMMT-H. Panels (a) and (b) show the storage modulus (E') and loss modulus (E''), respectively, as a function of frequency, while panel (c) shows the loss tangent ($\tan\delta$).

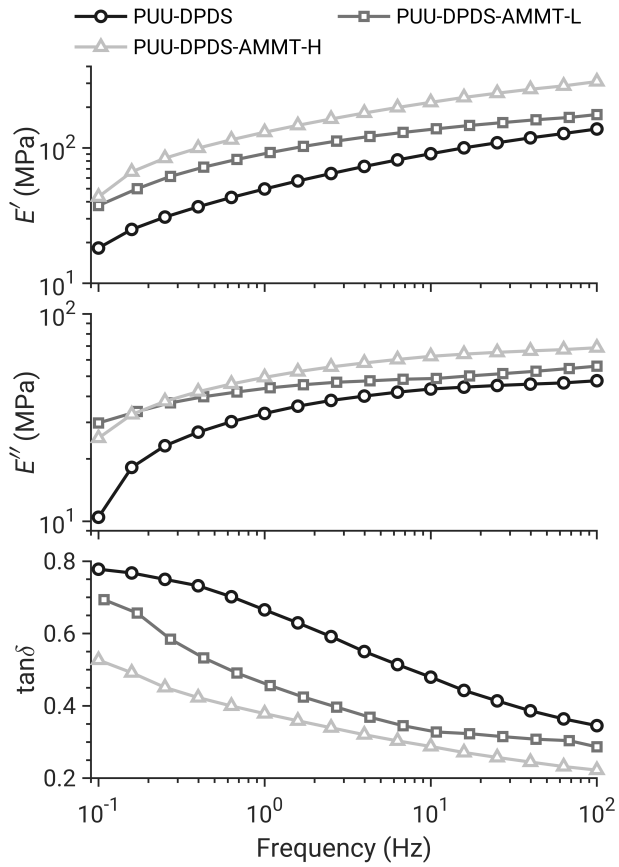

Fig. S5: Frequency-dependent viscoelastic properties of PUU-DPDS-based materials obtained from dynamic mechanical analysis. ◯ = PUU-DPDS, □ = PUU-DPDS-AMMT-L, △ = PUU-DPDS-AMMT-H. Panels (a) and (b) show the storage modulus (E') and loss modulus (E''), respectively, as a function of frequency, while panel (c) shows the loss tangent ($\tan\delta$).

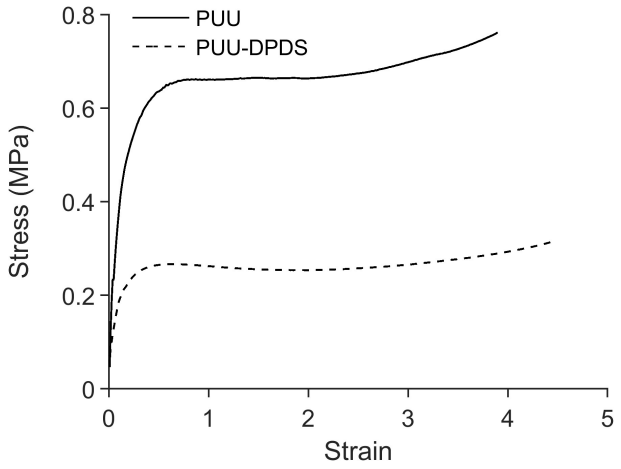

Fig. S6: Representative stress–strain curves for PUU and PUU-DPDS copolymer films tested at 25 °C under a 50 mm min^{-1} extension rate.

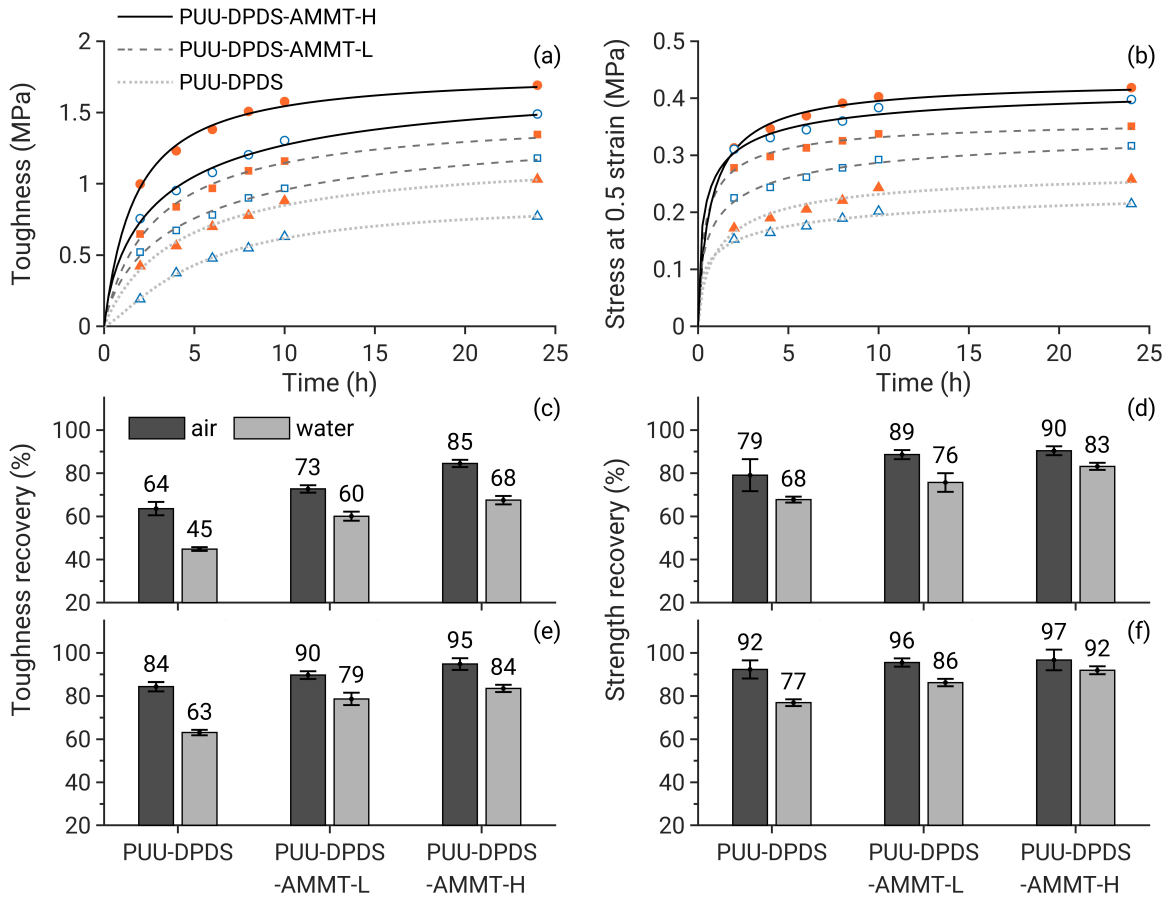

Fig. S7: Toughness and strength recovery of PUU-DPDS–based films during healing at 60 °C in air and underwater environments. ◯ = PUU-DPDS-AMMT-H, □ = PUU-DPDS-AMMT-L, △ = PUU-DPDS. Panels (a,b) show the time evolution of toughness and stress at a strain of 0.5 (taken as a measure of strength), respectively; blue unfilled symbols represent underwater healing, whereas orange filled symbols correspond to healing in air. Panels (c,d) show toughness and strength recovery after 8 hours, and panels (e,f) show recovery after 24 hours. Recovery in panels (c–f) is expressed as a percentage relative to the intact (uncut) specimen.

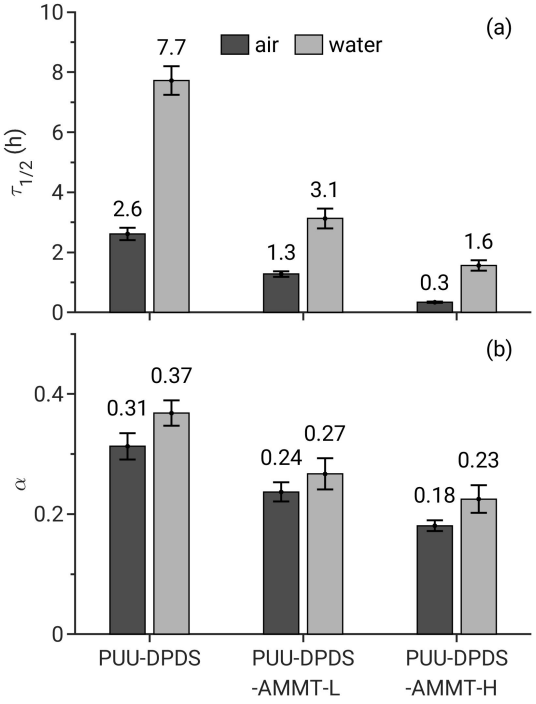

Fig. S8: Parameters (a) $\tau_{1/2}$ and (b) α of the power-law model for toughness recovery vs. time for PUU-DPDS, PUU-DPDS-AMMT-L, and PUU-DPDS-AMMT-H at 60 °C.

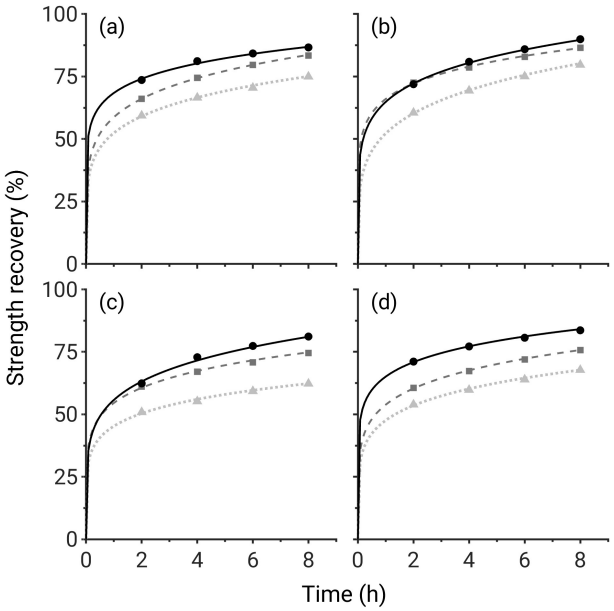

Fig. S9: Strength recovery (defined as the stress at a strain of 0.5) of cut samples healed under different conditions: (a) 30 °C in air, (b) 60 °C in air, (c) 30 °C in water, and (d) 60 °C in water. 100% corresponds to the strength of the intact (uncut) specimen. ◯ = PUU-DPDS-AMMT-H, □ = PUU-DPDS-AMMT-L, △ = PUU-DPDS.

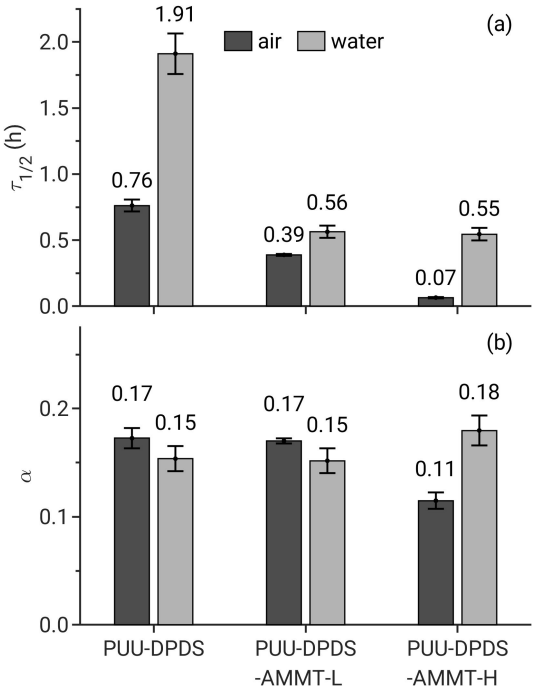

Fig. S10: Parameters (a) $\tau_{1/2}$ and (b) α of the power-law model for strength recovery vs. time for PUU-DPDS, PUU-DPDS-AMMT-L, and PUU-DPDS-AMMT-H at 30 °C.

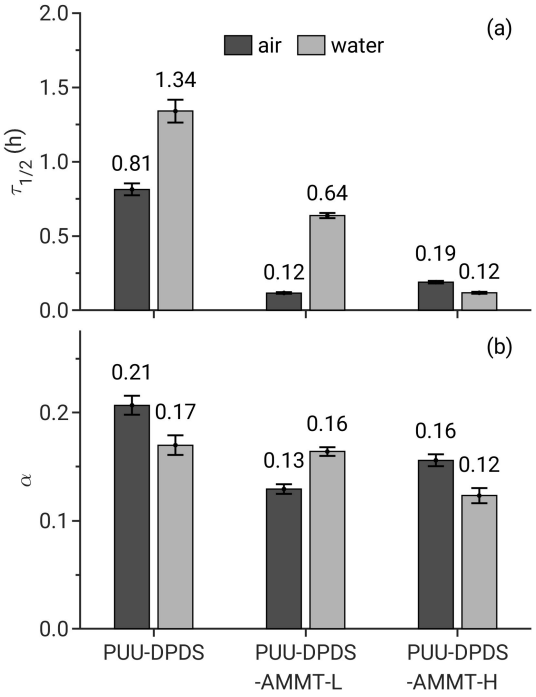

Fig. S11: Parameters (a) $\tau_{1/2}$ and (b) α of the power-law model for strength recovery vs. time for PUU-DPDS, PUU-DPDS-AMMT-L, and PUU-DPDS-AMMT-H at 60 °C.

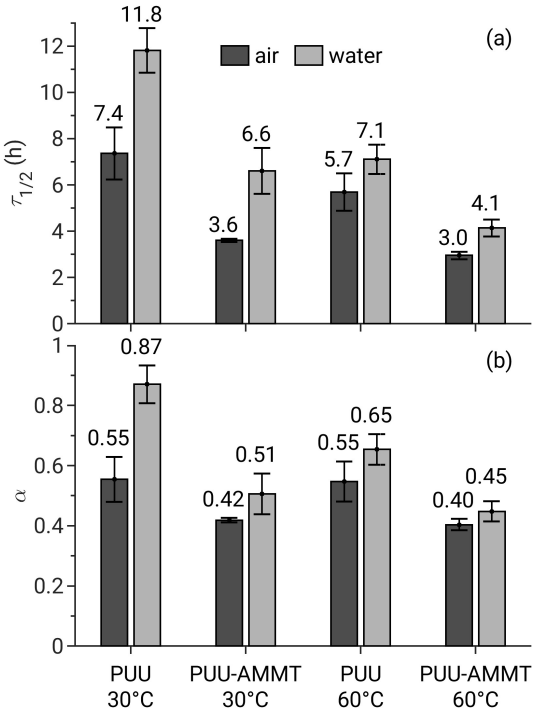

Fig. S12: Fitted parameters (a) $\tau_{1/2}$ and (b) α from the power-law model describing toughness recovery as a function of time for PUU and PUU-AMMT-H at 30 °C and 60 °C.

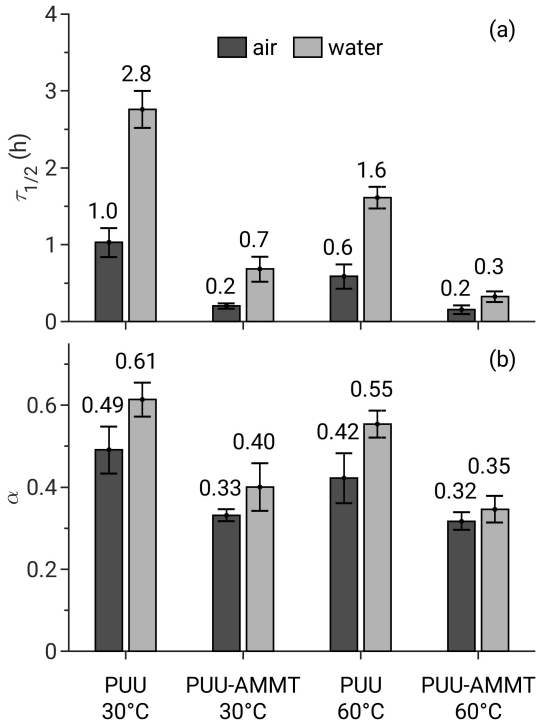

Fig. S13: Fitted parameters (a) $\tau_{1/2}$ and (b) α from the power-law model describing strength recovery as a function of time for PUU and PUU-AMMT-H at 30 °C and 60 °C.

Videos

Video S1. Self-healing of PUU and PUU-DPDS elastomers after cutting.

The specimens were cut with a razor blade and allowed to heal at room temperature for 24 h. The healed specimens were subsequently stretched manually to demonstrate recovery of mechanical integrity across the healed interface.

References

[1] George Odian. *Principles of Polymerization*. Wiley-Interscience, Hoboken, NJ, 4th edition, 2004.

[2] Charles M. Hansen. *Hansen Solubility Parameters: A User's Handbook*. CRC Press, Boca Raton, FL, 2nd edition, 2007.